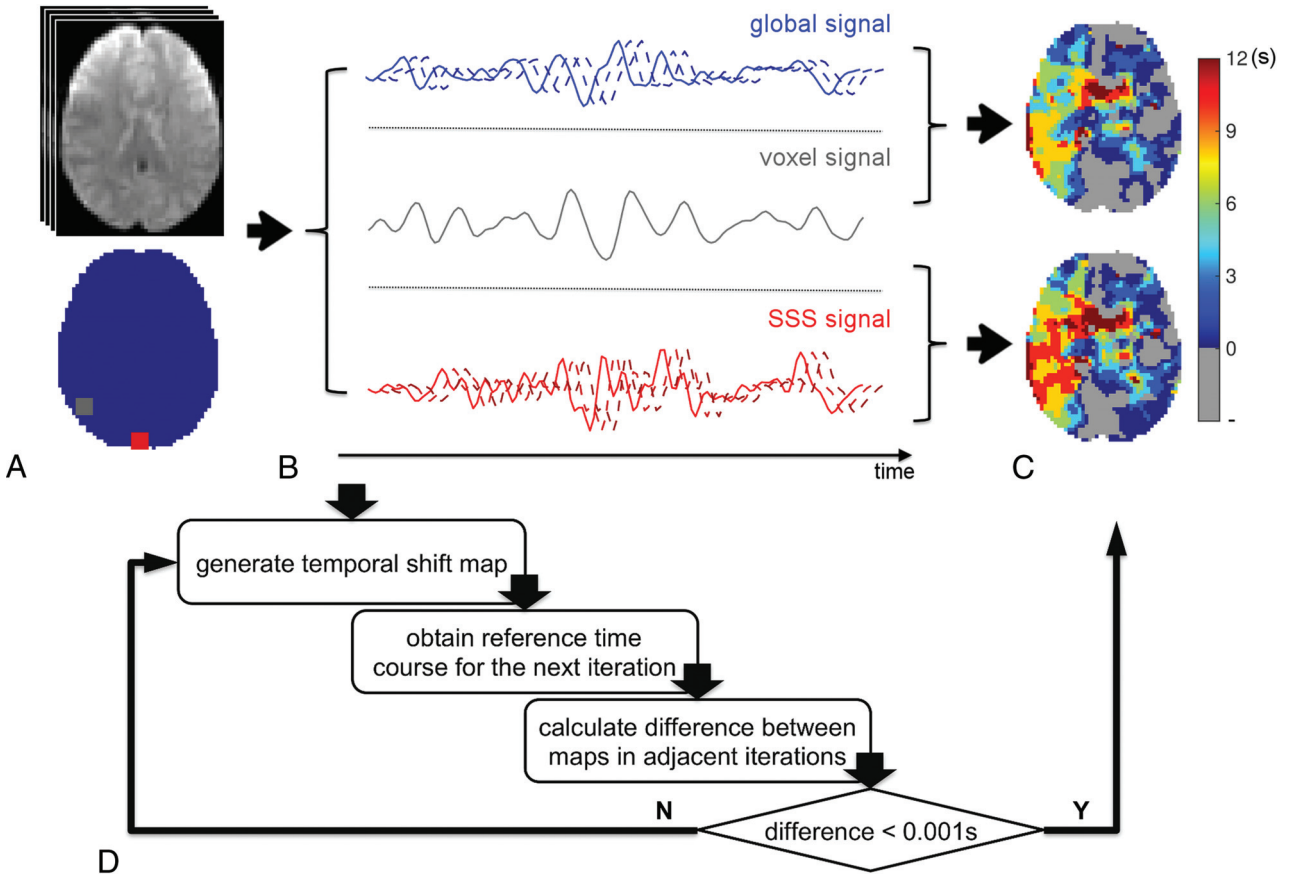

ON-LINE FIG 1. Schematic illustration of the procedure involved in temporal-shift analysis of resting-state BOLD data. *A*, The recorded BOLD images and brain mask are illustrated. *B*, After data preprocessing, the time course of each voxel was extracted. We considered 2 options for reference signals: the global mean signal and the superior sagittal sinus signal. The global mean signal was calculated by averaging the signals across the entire brain. The SSS signal was the mean signal over an ROI in the SSS. *C*, TS maps were created by determining a temporal offset that maximized the correlation coefficient between the time-shifted (−6 TR to +6 TR; ie, −12 seconds to +12 seconds) reference signal and the temporal signal of each voxel. The temporal offset was then assigned as the value of the respective voxel in the TS map. *D*, For SSS signal-based analysis, an iterative approach was used to optimize the calculation of TS maps. The average time evolution over voxels with zero time delay (offset = 0 second) from the previous iteration was calculated and used as the reference signal for the next iteration. The iteration was repeated until convergence so that the mean absolute difference between the TS maps in the successive iterations was lower than 0.001 second.

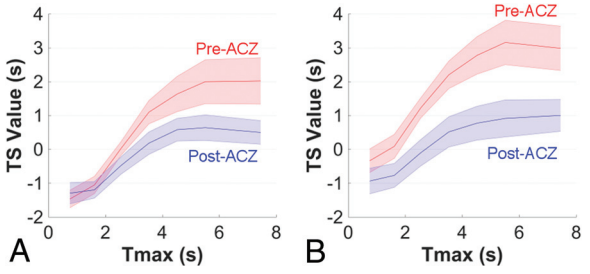

ON-LINE FIG 2. Correlation between the temporal-shift and T_{max} maps when using either the global (*A*) or the superior sagittal sinus (*B*) signal as the reference for calculating TS maps. Significant correlation was observed for both reference approaches (mixed-effects model, $P < .001$). The slopes of change in TS with respect to T_{max} were lower after acetazolamide administration when using the global signal ($P = .001$) and SSS ($P = .026$) as the reference signal, respectively. *Error bars* represent standard error of the mean.

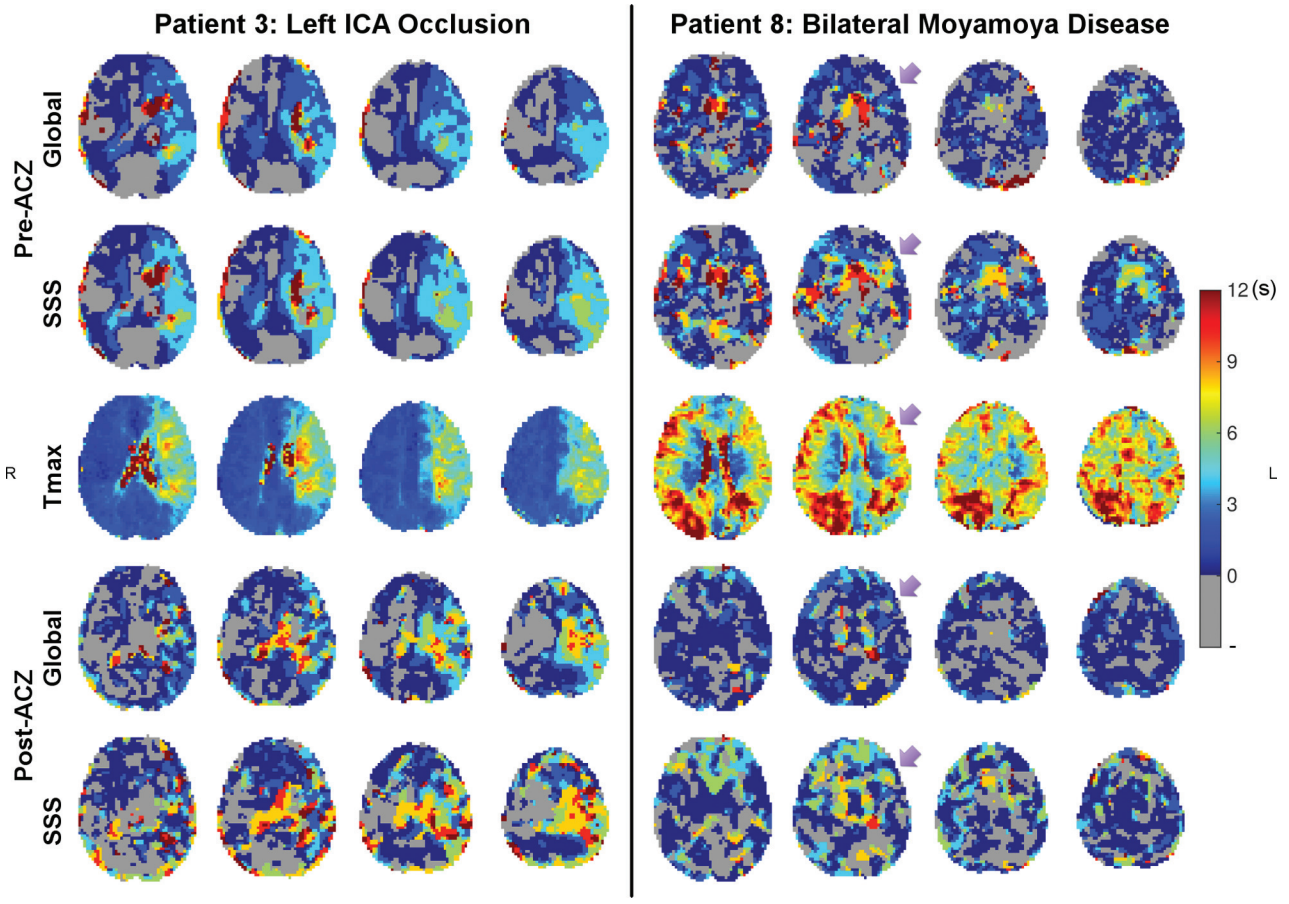

ON-LINE FIG 3. Temporal-shift maps derived from resting-state BOLD images (rows 1, 2, 4, and 5) and DSC T_{max} maps (row 3) in patients with severe unilateral (patient 3 with occlusion of left ICA) and severe bilateral (patient 8 with bilateral Moyamoya disease) diseases. TS maps exhibited a global resemblance to T_{max} maps. This agreement decreased after acetazolamide administration. Compared with using the global signal as a reference, TS maps generated with the superior sagittal sinus signal as a reference showed better agreement with T_{max} maps, particularly among patients with bilateral occlusion (*purple arrows*). The images are in radiologic convention.

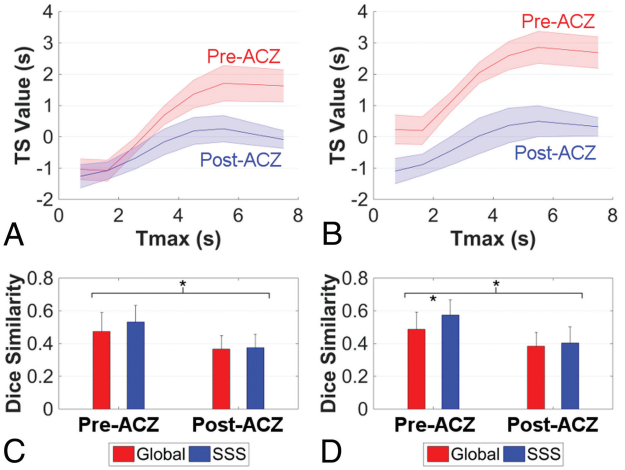

ON-LINE FIG 4. Correlation between the temporal-shift and baseline T_{max} maps when using either the global (*A*) or the superior sagittal sinus (*B*) signal as a reference for calculating TS maps. The mixed-effects model showed significant correlation for both reference approaches ($P = .009$ for the global signal; $P = .005$ for SSS). The slopes of change in TS with respect to baseline T_{max} were lower after acetazolamide administration when using the global signal ($P = .001$) and SSS ($P = .044$) as the reference signal, respectively. The mean Dice similarity coefficient between TS and baseline T_{max} maps by using $T_{max} > 4$ seconds (*C*) and $T_{max} > 3$ seconds (*D*) as criteria for defining hemodynamic compromise. The results derived from baseline T_{max} maps before ACZ challenge were similar to those with T_{max} maps after ACZ challenge (Fig 2 and On-line Fig 2). *Asterisks* indicate significant differences as determined by 2-way repeated-measures ANOVA with a post hoc Bonferroni-corrected paired *t* test.

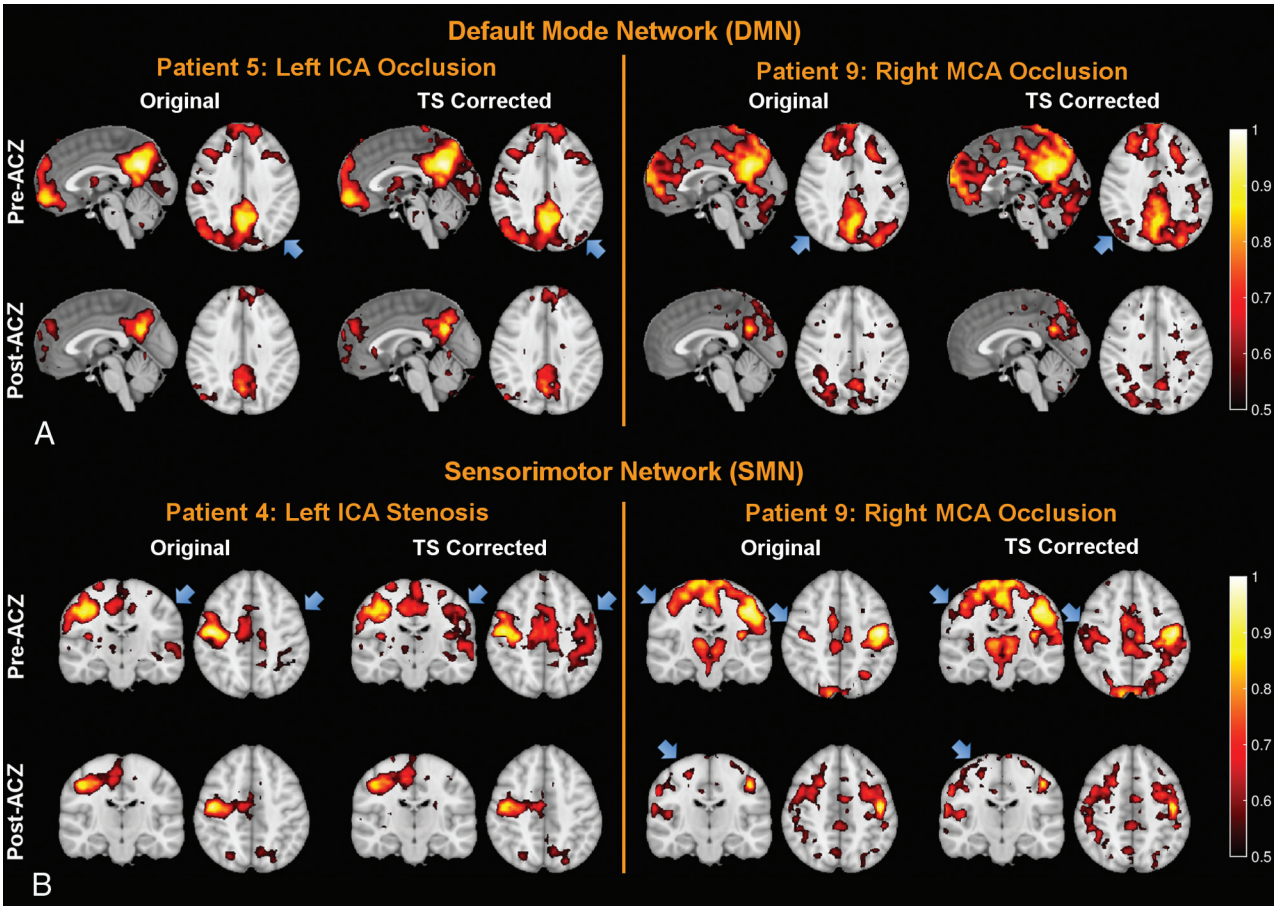

ON-LINE FIG 5. *A*, The default mode network in patients with severe unilateral disease (patient 5 with occlusion of the left ICA; patient 9 with occlusion of the right MCA). *B*, The sensorimotor network in patients with severe unilateral disease (patient 4 with stenosis of the left ICA; patient 9 with occlusion of the right MCA). Although functional connectivity changed after acetazolamide challenge, the DMN and SMN could be still identified. New network nodes were uncovered in the hypoperfused areas after the correction of time delay derived from temporal-shift analysis (see *blue arrows* in the original and TS-corrected networks). In general, these regions could be observed in the corresponding networks of healthy subjects. The images are in radiologic convention.

On-line Table: Summary of patient data

Patient No.	Age (yr)/ Sex	Diagnosis	Overlap[a] (T_{max} >4 sec as a Criterion for Hypoperfusion)				Overlap[a] (T_{max} >3 sec as a Criterion for Hypoperfusion)			
			Pre-ACZ		Post-ACZ		Pre-ACZ		Post-ACZ	
			Global	SSS	Global	SSS	Global	SSS	Global	SSS
1	58/F	Left-sided Moyamoya disease	0.431	0.429	0.406	0.379	0.510	0.533	0.523	0.565
2	43/F	Occlusion of the right MCA	0.331	0.380	0.304	0.310	0.310	0.418	0.376	0.438
3	70/F	Occlusion of the left ICA	0.765	0.751	0.615	0.568	0.746	0.765	0.633	0.623
4	38/F	Stenosis of the left ICA	0.532	0.574	0.375	0.337	0.491	0.542	0.346	0.320
5	45/M	Occlusion of the left ICA	0.645	0.646	0.328	0.313	0.616	0.667	0.383	0.376
6	67/M	Occlusion of the right ICA	0.490	0.518	0.393	0.402	0.522	0.611	0.412	0.426
7	40/F	Bilateral Moyamoya disease	0.370	0.482	0.389	0.400	0.419	0.624	0.407	0.444
8	32/F	Bilateral Moyamoya disease	0.483	0.632	0.317	0.468	0.484	0.632	0.318	0.474
9	54/F	Occlusion of the right MCA	0.676	0.662	0.258	0.241	0.665	0.696	0.310	0.298
10	60/M	Occlusion of the left ICA	0.333	0.411	0.383	0.324	0.369	0.461	0.337	0.301
11	31/F	Stenosis of the left ICA	0.322	0.337	0.251	0.220	0.469	0.486	0.344	0.285
12	32/F	Bilateral Moyamoya disease	0.448	0.460	0.321	0.352	0.494	0.521	0.347	0.374
13	63/F	Stenosis of the left ICA	0.663	0.657	0.627	0.522	0.604	0.723	0.560	0.410
14	39/F	Occlusion of bilateral ICA	0.323	0.376	0.429	0.536	0.355	0.395	0.440	0.561
Mean (SD)			0.487 (0.150)	0.523 (0.131)	0.385 (0.113)	0.384 (0.107)	0.504 (0.122)	0.577 (0.115)	0.410 (0.098)	0.421 (0.106)

[a] Spatial overlap of delay coverage between DSC T_{max} maps and temporal-shift maps as evaluated by the Dice similarity coefficient.